

A PHYSICAL MODEL FOR MUSCULAR BEHAVIOR

JULIA T. APTER *and* WILLIAM W. GRAESSLEY

From the Section of Mathematical Biology, Division of Surgery, Presbyterian-St. Luke's Hospital, Department of Surgery, University of Illinois, Chicago, Illinois 60612 and the Department of Chemical Engineering, Northwestern University, Evanston, Illinois 60201

ABSTRACT A model for muscular behavior has been developed by a generalization of the laws governing the viscoelastic behavior of polymeric materials. The model simulates events thought to take place during stretch, loading, and stimulation of muscle, whether smooth or striated. The equations of motion were solved with an analogue computer for several types of perturbation, and stress, strain, and strain-rate curves were generated. Model parameters were selected by fitting experimental stress-relaxation data. The resulting equations predicted the frequency dependence of dynamic modulus and phase angle within experimental error. With appropriate boundary conditions and suitable values for model parameters, the computed results also closely resembled experimental curves of contraction velocity vs. time, isometric tension development vs. time, force-velocity curves, and temperature-tension relationships. These results call attention to the relationship between the behavior of various kinds of muscle and open the way for quantifying muscular behavior in general.

INTRODUCTION

Among models of muscular behavior are Hill's contractile element (1938), Huxley's sliding filament hypothesis (1957), Bahler's force generator (1968), and the variable viscosity dashpot of Vickers and Sheridan (1968). The contractile element makes it possible to quantify force-velocity curves; the sliding filament hypothesis quantifies a length-active tension relationship; the force generator analyzes isometric tension development following repetitive stimulation; the variable dashpot calls attention to dependence of force-velocity curve parameters on stimulus level. However, a wide variety of muscular behavior is not contained within any of these models. Examples are stress relaxation and recontraction following a step-function strain, creep of a loaded muscle, stress response to a sinusoidal strain, the deviation of force-velocity curves from a hyperbolic form under some circumstances. Moreover, none of the models, even one (Bahler, 1968) which fits the time course of stress development of a stimulated loaded muscle, can match the velocity-time curve for the shortening of muscle.

What is needed is a model with mechanical properties derived from the physical and chemical changes underlying muscular contraction, and yielding muscular

responses to any feasible forcing. This level of description is not yet achievable primarily because the detailed mechanism of excitation-contraction coupling is still open to debate. However, we have found it possible to develop an intermediate model suggested by events already known to occur, albeit slowly, in viscoelastic, inert polymers (Tobolsky, 1960). This model appears to be an improvement over previous models since it represents a wider range of muscular characteristics. It is not intended as a molecular theory of muscular contraction, but as a tool for classification, quantification, and design of experiments.

METHODS

Model

Muscle, whatever its contractile state, is always viscoelastic; that is, some work done in stretching muscle is dissipated as heat and some is conserved and recoverable. The dissipative property of any material can be characterized by one or more viscosity coefficients η_i . Similarly, the conservative behavior is represented by one or more elastic moduli E_i . Muscle in stress relaxation experiments displays both an instantaneous modulus and an equilibrium modulus, so a three parameter viscoelastic model (η , E_1 , E_2) is the simplest possible description available (Fig. 1) (Apter, Rabinowitz, and Cummings, 1966). The mechanical response is given by the following equation (Kolsky, 1960):

$$\sigma + \frac{\eta}{E_2} \dot{\sigma} = E_1 \epsilon + (E_1 + E_2) \frac{\eta}{E_2} \dot{\epsilon}, \tag{1}$$

where σ is stress and ϵ is strain, defined as

$$\epsilon = \frac{l - l_0}{l_0}, \tag{2}$$

with l being the existing length and l_0 the *instantaneous* unstretched length of the muscle. Variability in l_0 incorporates the fact familiar to physiologists that muscle may have a range of unstretched lengths, depending on its contractile state. Inertial terms have been omitted to

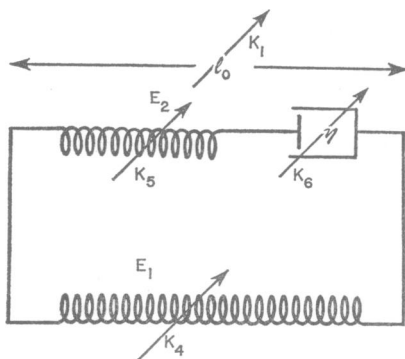


FIGURE 1 Viscoelastic model of muscular "contractile elements." It includes a Maxwell element in parallel with a spring, all elements having variable parameters E_1 , E_2 , and η . The k_i ($i = 1, 4, 5, 6$) of equations 7-9, corresponding to a particular parameter are noted.

keep the analysis simple. In general, it is possible to design experiments to minimize inertial contributions, or to account for them on an *ad hoc* basis.

Let us now suppose that the values of E_1 , E_2 , η , and l_0 depend on the macromolecular arrangement, which in turn is influenced by substances whose entry rates into the system depend to some extent on the strain. Specifically for muscle we assume that the state of contraction depends on some substance N near the intracellular macromolecules. We also assume that n , the concentration of N, varies with time according to

$$\dot{n} = k_2\epsilon - k_3n + S(t). \quad (3)$$

The term on the left is the time rate of change of n within the cell. The first term on the right corresponds to a diffusion of N into the cell at a rate proportional to the strain. This would happen if strain physically increases membrane permeability by opening "pores." The rate constant k_2 is defined as per unit external concentration of N. The second term corresponds to deactivation or removal of N from within the cell at a rate proportional to its internal concentration. The rate constant is k_3 . The third term represents the influx as a result of membrane depolarization from electrical or chemical stimulation. Suppose stimulation begins at time t_0 and continues until t_1 . For this case we have chosen the following simple form for $S(t)$:

$$\begin{aligned} S(t) &= 0 & 0 < t < t_0 \\ &= k_7 & t_0 < t < t_1 \\ &= 0 & t_1 < t < \infty, \end{aligned} \quad (4)$$

in which k_7 is a constant. Thus, according to this view, stimulation corresponds to a constant rate of admittance of N to the cell.

The instantaneous rest length and the viscoelastic parameters of muscle are taken to be the following simple functions of concentration n :

$$l_0 = l_0^\infty + \frac{l_0^0 - l_0^\infty}{1 + k_1 n} \quad (5)$$

$$E_1 = E_1^\infty - \frac{E_1^\infty - E_1^0}{1 + k_4 n} \quad (6)$$

$$E_2 = E_2^\infty - \frac{E_2^\infty - E_2^0}{1 + k_5 n} \quad (7)$$

$$\eta = \eta^\infty - \frac{\eta^\infty - \eta^0}{1 + k_6 n}, \quad (8)$$

with the superscripts 0 and ∞ referring to completely relaxed ($n = 0$) and completely contracted ($n = \infty$) states, respectively. Thus, the moduli and viscosity increase with n and the rest length decreases, just as observed during muscular contraction (Ramsey and Street, 1940; Apter, Rabinowitz, and Cummings, 1966).

In summary, this model represents muscle, whatever its level of contraction, as a three parameter viscoelastic solid (Staverman and Schwarzl, 1956). The unique energy-producing (or converting) characteristic of muscle has been embodied by allowing these parameters to depend on the level of some chemical in the environs of the macromolecules responsible for

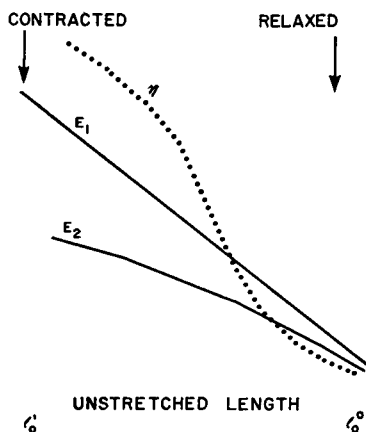


FIGURE 2 Empirical qualitative relation between E_1 , E_2 , and η and the unstretched length l_0 which is proportional to contractile state $C = (l_0 - l_0^{\infty}) / (l_0^0 - l_0^{\infty})$. (See Glossary.)

the viscoelastic properties. Thus, muscular contraction is represented simply by variations in viscosity, moduli, and rest length of the muscle.

All these equations have specific physiological counterparts as well. The fact that E_1 , E_2 , and η depend on contraction level reflects the experimental data on viscoelastic responses of excised muscle (Ramsey and Street, 1940; Sandow, 1965; Apter et al., 1966; Apter and Graessley, 1969). In our view equation 3 represents a highly simplified description of the events known as muscular excitation-contraction coupling (Sandow, 1965). This equation is probably the simplest formalism consistent with current understanding: ions such as K^+ , Na^+ , and Ca^{++} enter the muscle cell through its membrane during stimulation or enter through membrane pores created or enlarged when the muscle is stretched. The removal term could be binding of ions by sarcoplasmic reticulum or exit of ions by pumping through the cell membrane. Equations 5-8 incorporate the events known as the "sliding filament hypothesis" of muscular contraction (Huxley, 1957, 1963). The rearrangement of actin and myosin that takes place as muscle shortens (or as l_0 decreases) is assumed here also to be associated with increases in E_1 , E_2 , and η . Their interrelation is shown in Fig. 2, which is compiled from experiments on smooth muscle (Apter et al., 1966; Apter and Marquez, 1968 *a* and *b*).

The precise form of equations 5-8 is arbitrary, and chosen for simplicity. An exponential or even a linear (rather than hyperbolic) relation would also have given a reasonable representation of the data in Fig. 2. Some justification for the particular form selected, however, can be elicited from the following argument (Apter, 1961).¹

Suppose the stimulant, N , is taken to be a single factor which acts on a single muscle component A . Consider an equilibrium between N , free activator A , and a bound activator NA :



with an equilibrium constant, K . The equilibrium activities (A) and (NA) are

$$(A) = A_0 / (1 + kn) \quad (10)$$

$$(NA) = kn(A) = knA_0 / (1 + kn), \quad (11)$$

with $k = K^{-1}$ and $(N) = n$. A_0 is the total available amount of activator. Let the elastic param-

¹ Suggested by H. D. Landahl.

eters $E(E_1$ or E_2 or l_0 or η) be a linear combination of the activities (A) of the free and (NA) of the bound activator; i.e.,

$$E_1 = \alpha_4(A) + \beta_4(NA) = \frac{\alpha_4 A_0}{1 + kn} + \frac{\beta_4 kn A_0}{1 + kn}, \quad (12)$$

or

$$E_1 = \beta_4 A_0 + \frac{(\alpha_4 - \beta_4) A_0}{1 + kn}. \quad (13)$$

Comparing equation 13 with equation 6, we see that

$$E_1^0 = \alpha_4 A_0; \quad E_1^\infty = \beta_4 A_0. \quad (14)$$

The simplest model, then, would have

$$k_1 = k_4 = k_5 = k_6 = K^{-1}, \quad (15)$$

and therefore all the k_i would be related to the equilibrium constant of equation 9.

How this system is able to generate mechanical energy is best seen by an example. Consider a "muscle" initially stretched to l by some external agency, and held at l until the stress becomes constant. The unstrained length decreases smoothly from its longest or "relaxed" value l_0^0 to a shorter or more contracted unstrained length l_0 as n builds up. Eventually, n levels off at a value appropriate to the static strain ϵ . Note that the external or apparent strain ϵ_a is $(l - l_0^0)/l_0^0$ while the internal strain ϵ , which controls the level of N , is larger, being $(l - l_0)/l_0$ as given by equation 2. Now superimpose a small oscillatory strain and examine the changes during one cycle. In the rising portion of the cycle, work is done by the external agency on the

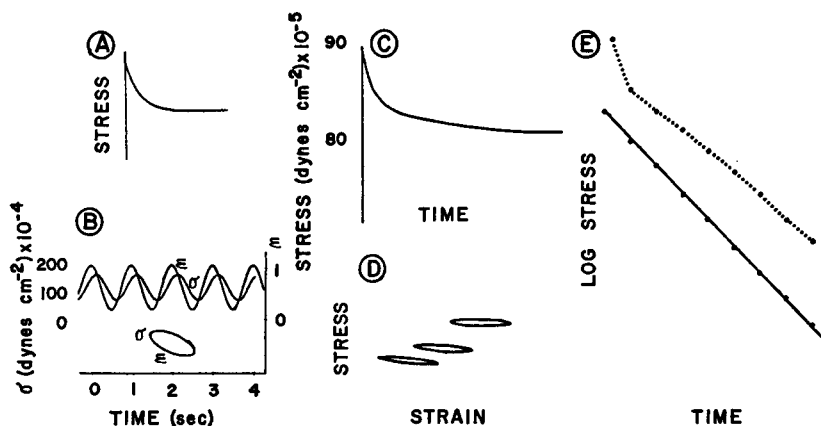


FIGURE 3 Stress responses of the model, when k_2 of equation 4 vanishes, to a step-function strain and to a sinusoidal strain. The stress relaxation (A) and stress-strain loop (B) shown are characteristic also of elastin, an amorphous polymer (whose behavior is shown in [C] and [D]). Stress relaxation for the model and elastin can be described with a single time constant η/E_2 , which is the slope of the linear plot of log stress vs. time in (E), where the dotted line was taken from the elastin curve in (C) and the solid line from the model curve in (A).

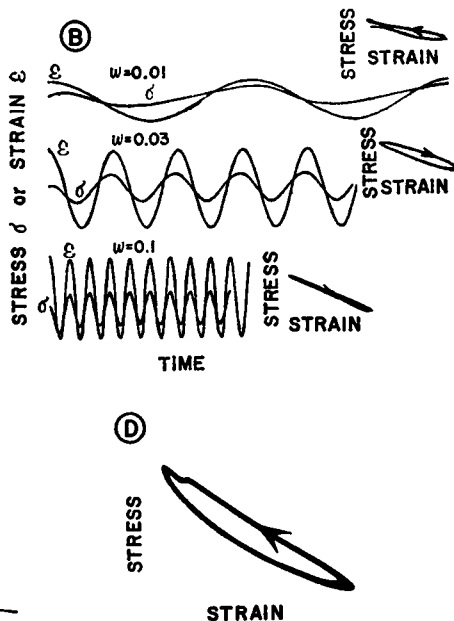
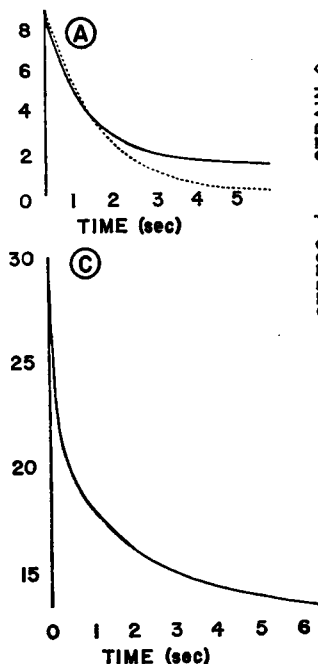
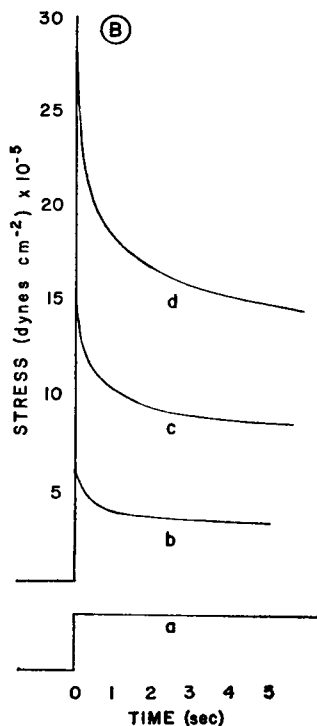
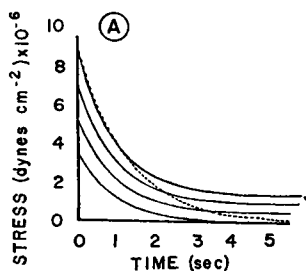


FIGURE 4

FIGURE 5

FIGURE 4 (A) Response of model with parameters (Table I) chosen to match those of Fig. 5 to several step-function increases in length. For comparison a dashed line simple exponential (described by a single time constant) is included. Note that the stress does not fall nearly so fast as a simple exponential. A plot of these data as log stress vs. time deviates considerably from a straight line. The specimen was found to be Hookian in behavior making the model E_1 constant since E_1 was obtained empirically. (B) Tracings (b), (c), and (d). Response of urinary bladder of dog in Ca-free Ringer's solution containing EDTA always stress-relaxes without recontraction, whatever the strain level. These curves also cannot be described by a single time constant. Tracing (a) shows the time course of the step-function strain.

FIGURE 5 Response of the model when parameters were chosen to make the model behave like smooth muscle in the absence of a stimulant. See Table I for all parameter values. (A) shows the stress relaxation which follows each step function strain taking place at $t = 0$ at the high ϵ levels tested. These curves are not describable by a single time constant as shown by the dashed line which is a perfect exponential curve. (B) shows the response of the model to oscillation at several frequencies. Nonlinearity is recognized at the lowest frequency where the sinusoidal strain produces a stress which is not truly sinusoidal. This frequency is also associated with a positive phase shift in the stress-strain loop, but there was no elastic modulus enhancement at any frequency tested.

Response of urinary bladder muscle in Ca-free EDTA solution resembles the model with this set of parameters as (C) shows: i.e. stress relaxation with a recontraction; and D shows the response to oscillation at $\omega = 0.02$ Hz.

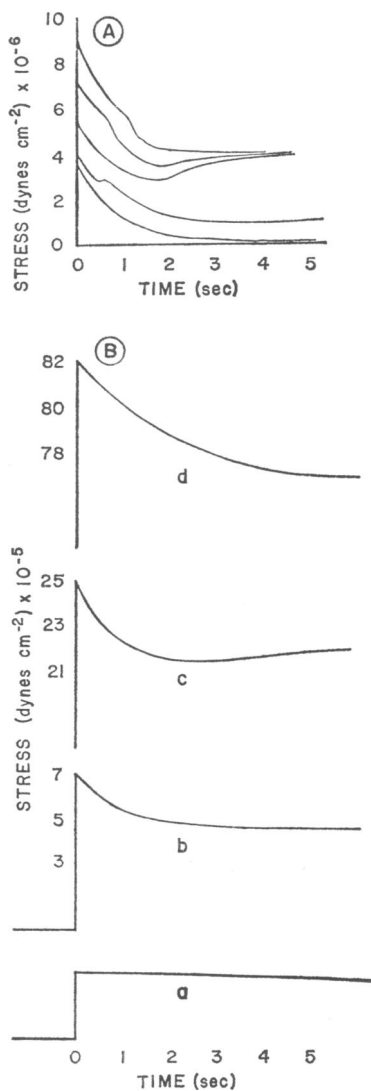


FIGURE 6

FIGURE 6 (A) Response of the model with parameters chosen to match those of Fig. 7 to several step-function increases in length. There is evidence of recontraction at all levels tested, but most marked at intermediate strains. The model is not developed to predict a certain elastic modulus from a given strain level. Rather these are empirically determined from data like these and are illustrated in Fig. 2. Length changes can be computed from values in Table I and the peak tension which gives $E_1 + E_2$ directly. (B) Response of urinary bladder of dog in Ringer's solution containing 10 $\mu\text{g/ml}$ of bethanechol chloride. Three strain levels were used to show simple stress relaxation at low (b) and very high (d) strains, with recontraction at intermediate strains (c). The erratic early recontractions characteristic of the model's response (A) could not be found in real muscle. (a) shows the time course of the step-function strain.

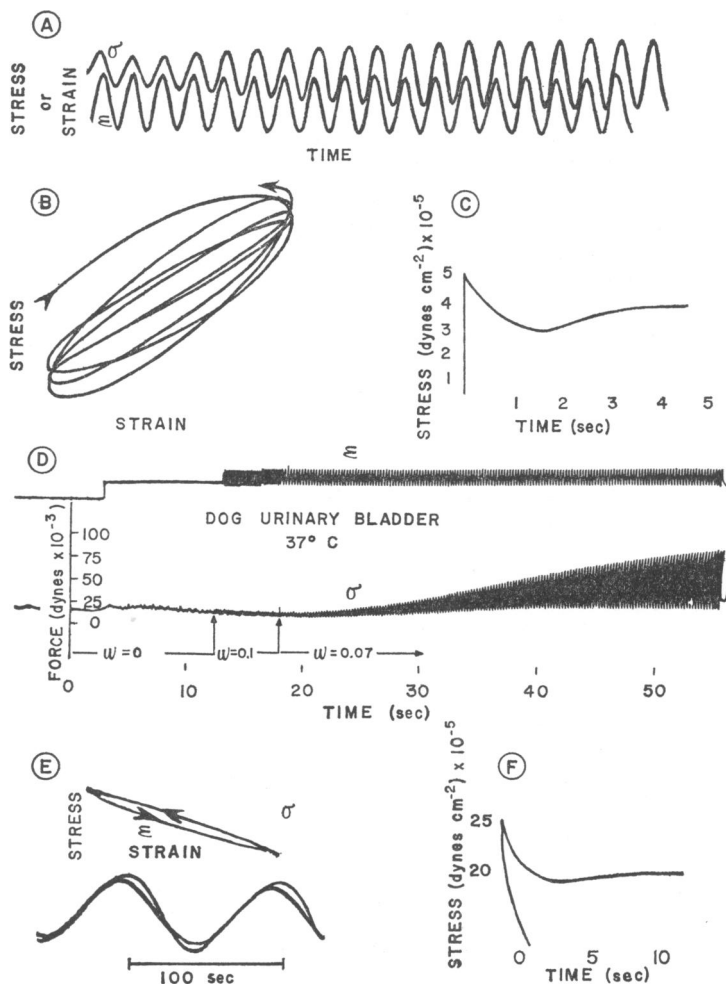


FIGURE 7

FIGURE 7 (A), (B), and (C) show stress response of the model when parameters were chosen to make the model behave like smooth muscle in the presence of a stimulant; (see Table I for parameter values). Response to a sinusoidal forcing depends on frequency and is nonlinear at low frequencies. (A) and (B) show a phase lag and stress-relaxation for the first few oscillations. Then there is a phase lead accompanied by an increase in elastic modulus as shown by an increase in the amplitude of σ even though ϵ remains constant. (C) is an example of the model's response to a step-function intermediate strain showing recontraction. (D), (E), and (F) show the corresponding stress response of urinary bladder in the presence of bethanechol chloride. All real muscular responses resemble those of the model except in so as the model starts out with $n = 0$ at t_0^0 to explain the initial transient phase lag which was far not found in real muscle.

muscle. The component N diffuses into the muscle, increasing E_1 , E_2 , and η and decreasing l_0 . In the falling portion of the cycle, ϵ decreases and the muscle does work on the external agency. In an ordinary viscoelastic solid the flow of mechanical energy is less in the falling portion; in a perfectly elastic body it is the same. In this model, however, the flow of energy is greater than in the rising part of the cycle because the concentration of N is higher. The external stress is therefore greater both because internal strain is larger and because E_1 and E_2 are larger. As a consequence, in this system strain can lead stress, whereas strain lags behind stress in an ordinary viscoelastic material.

Clearly the generation of power depends on frequency in oscillatory situations. If oscillations are sufficiently slow, the concentration of N will be in step with the strain and the muscle will be dissipative because of its viscosity term. Likewise, at sufficiently high frequencies the concentration of N will be unable to respond to the changes in strain and no net energy will be produced. Only at some intermediate range of frequencies will a substantial phase lead appear. In this range the muscle will convert chemical energy associated with the diffusion process into mechanical energy.

Experiments on Muscles

Experiments on real muscles were restricted to those for which our laboratories are fully equipped for quantitative analysis. These consist in imposing a step-function stretch to give stress relaxation curves and a sinusoidal stretch over frequencies from 0.01 to 2 Hz to give dynamic modulus and phase angle. The object was to obtain model parameters from stress-relaxation curves of a given muscle, then to compare experimental behavior in oscillatory experiments with results computed from the model. In addition, the model was used to produce, among other things, force-velocity curves (Fenn and Marsh, 1935; Wilkie, 1949), isometric tension response (Buller and Lewis, 1965), and a temperature-tension relationship (Apter and Marquez, 1968 *a* and *b*; Apter and Najafi, 1968). All calculations were performed by analogue computer. Computer outputs were compared with the reported behavior of real muscle.

All specimens were obtained from recently sacrificed anesthetized animals and were prepared as ring or slitted segments supported horizontally on two hooks in an environment suitable for the particular specimen. The methods are described in detail in previous work from this laboratory (Apter et al., 1966; Apter and Marquez, 1968 *a* and *b*). Smooth muscles were studied in the form of urinary bladder, aortic wall, pulmonary artery wall, iris sphincter, and ciliary muscles from dog, cat, and guinea pig. Striated muscle specimens were taken from the cat gastrocnemius and from the heart of cats, dogs, rabbits, and guinea pigs. No effort was made at this time to distinguish among the various animals, all of which were also used by other experimenters for other purposes.

Unless otherwise specified, all specimens were tested at 37°C in Ringer's solution, Tris buffered to pH 7.2. Phenylephrine hydrochloride in concentrations of 4 $\mu\text{g/ml}$ was used to contract or "stimulate" arterial smooth muscles; acetylcholine at 10 $\mu\text{g/ml}$ was used to contract iris sphincter. Bethanechol chloride in concentrations of 10 $\mu\text{g/ml}$ was used to contract or stimulate urinary bladder muscle. Cardiac and striated muscles were studied also in Ca-free Ringer's solution containing EDTA at 0°C to retard development of rigor mortis (Apter and Najafi, 1968), although it was impossible to prevent it altogether during a study of the frequency dependence of viscoelasticity.

The specimens were stretched to 6 or 7 strain levels (2, 12, 20, 51, 70, 82, 100%) by separating the hooks to register an initial mean force at a steady length $l > l_0^0$. Step-function strain of from 1% to 100% over mean strain was imposed within 17 msec by moving one supporting

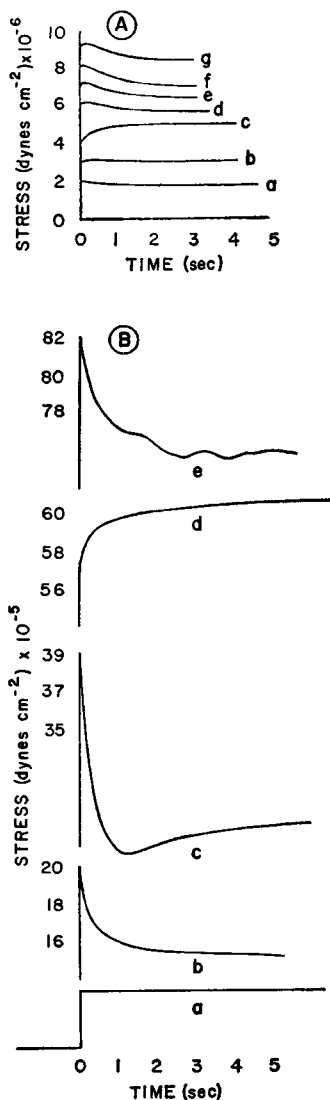


FIGURE 8 (A) Response of the model with parameters chosen to match those of Fig. 12 to several step-function increases in length. Stress relaxation occurs at low and at high strains. Contraction alone occurs at intermediate strains and reconstrictions are superimposed at moderately low and high strains. Since the equilibrium modulus E_1 of the model was obtained from the experimental stress-relaxation curves, naturally the strain associated with a given response is not pertinent and cannot be predicted from the model. The peak tension and $E_1 + E_2$ from Table I gives the actual strain level. (B) Response of the left ventricle of rabbit heart strained to four levels to show (from low to high strains): (b) simple stress relaxation, (c) stress relaxation with small recontraction, (d) recontraction without stress relaxation, (e) reconstrictions superimposed on stress relaxation. (a) shows the time course of the step-function strain. The values in Table I were obtained from fitting these curves.

hook attached to a vibration exciter activated by an electronic square wave generator. This changed the specimen suddenly (step-function) from one nonzero strain level to another to produce stress-relaxation curves of the form shown in Fig. 4, 6, and 8. The vibration exciter was then activated by a sinusoidal electronic output to oscillate the already stretched specimen at frequencies from 0.01 to 2 Hz (Apter and Marquez, 1968 *b*). The movement of the stretching hook was monitored by a photosensor displacement transducer (frequency response 11,000 Hz). The other hook was coupled to a force transducer (frequency response 350 Hz). Outputs were plotted as functions of time on an ink writer recorder and were imaged as stress vs. strain on a storage cathode ray tube oscilloscope. Dynamic modulus and phase angle were calculated at each frequency.

Stress relaxation curves were compared with the computer solution of the model to a step-function forcing by varying E_1 , E_2 , η , and the k_i until a good match resulted. Initial estimates for $E_1 + E_2$ came from the peak tension, for E_1 from the steady-state tension, and for E_2/η from the time to go from peak to steady state. However, except for elastin (Fig. 3), the relaxation was never a single time-constant exponential and in some cases was followed by recontraction, so no combination of E_1 , E_2 , and η alone could match the stress-relaxation curve of a viable muscle. Nonzero values of the k_i in addition to E_1 , E_2 , and η were thus required to fit the experimental curves. In effect, the order of magnitudes of the k_i were controlled by the time for relaxation while the ratio k_2/k_3 depended on the amount of the recontraction (Fig. 4, 6, and 8).

RESULTS

Examples of experimental data and the computer-generated stress-relaxation curves are shown in Fig. 4–8. The final values of E_1 , E_2 , η , and the k_i are given in Table I. With the number of adjustable parameters it is of course not surprising

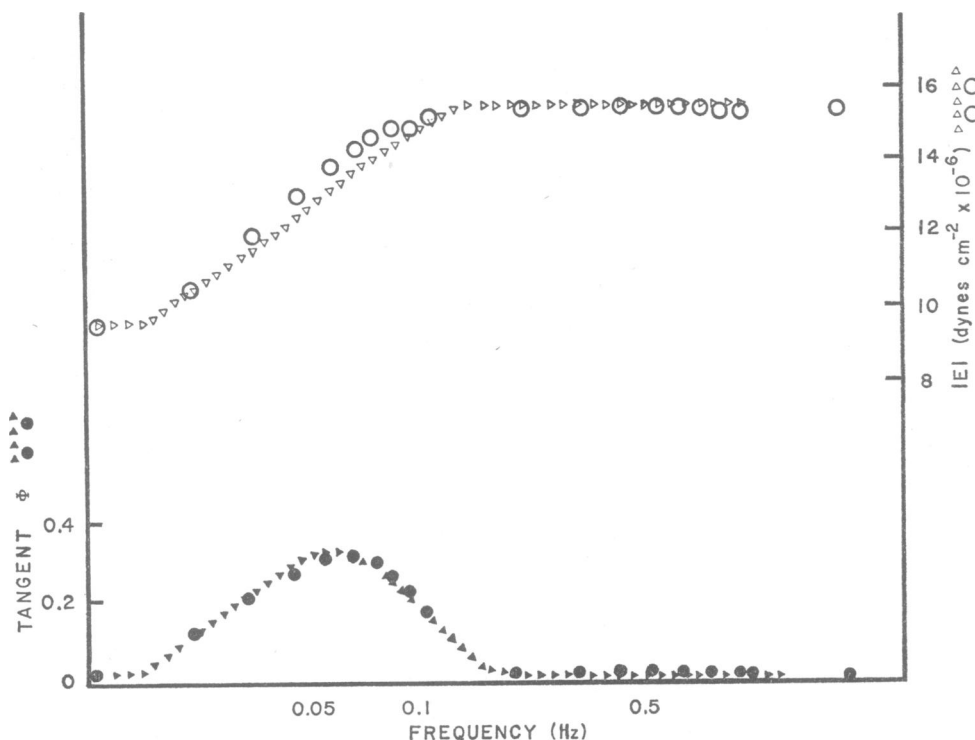


FIGURE 9 Experimental data obtained from same specimen as in Figs. 10 and 11, but 24 hr after removal from the dog and with demonstrably dead muscle since it did not respond to a stimulant. The match of data and model curves is well within experimental error (Apter et al., 1966). This is not surprising since the stress-relaxation curve was clearly exponential so that parameter estimation gave reliable values for E_1 , E_2 , and η , with all $k_i = 0$ (Apter and Marquez, 1968 b).

TABLE I

Modeled material	Temp.	k_1	k_2	k_3	k_4	k_5	k_6	E_1	E_1^0	E_1^∞	E_2	E_2^0	E_2^∞	η	η^0	η^∞	l_0/l_0^∞
	°C			sec						dynes $\text{cm}^{-2} \times 10^{-8}$				poise $\times 10^{-3}$			
Elastin	37	0	0	0	0	0	0	50	10	0.5	1			10			
Relaxed smooth muscle	37	0.1	0.2	0.8	0.1	0.1	0.1										1.85
Contracted smooth muscle	37	0.1	0.5	0.4	0.1	0.1	0.1			50			7			160	1.85
	0	0.07	0.4	0.2	0.07	0.07	0.07			5.9			7.6			181	1.70
Striated muscle	37	0.75	0.9	.15	1.0	1.0	1.0		10	50	1	7			10	160	2.0

Superscript 0 refers to relaxed muscle.

Superscript ∞ refers to contracted muscle.

that the experimental curves could be matched with great precision. The remarkable result is the quantitative agreement, with no additional adjustment of the parameters, between experimental and computer curves for oscillatory response (Fig. 9-11). Both the frequency dependence of the absolute dynamic modulus and the phase shift are accurately predicted, including the change from a phase lead to a phase lag

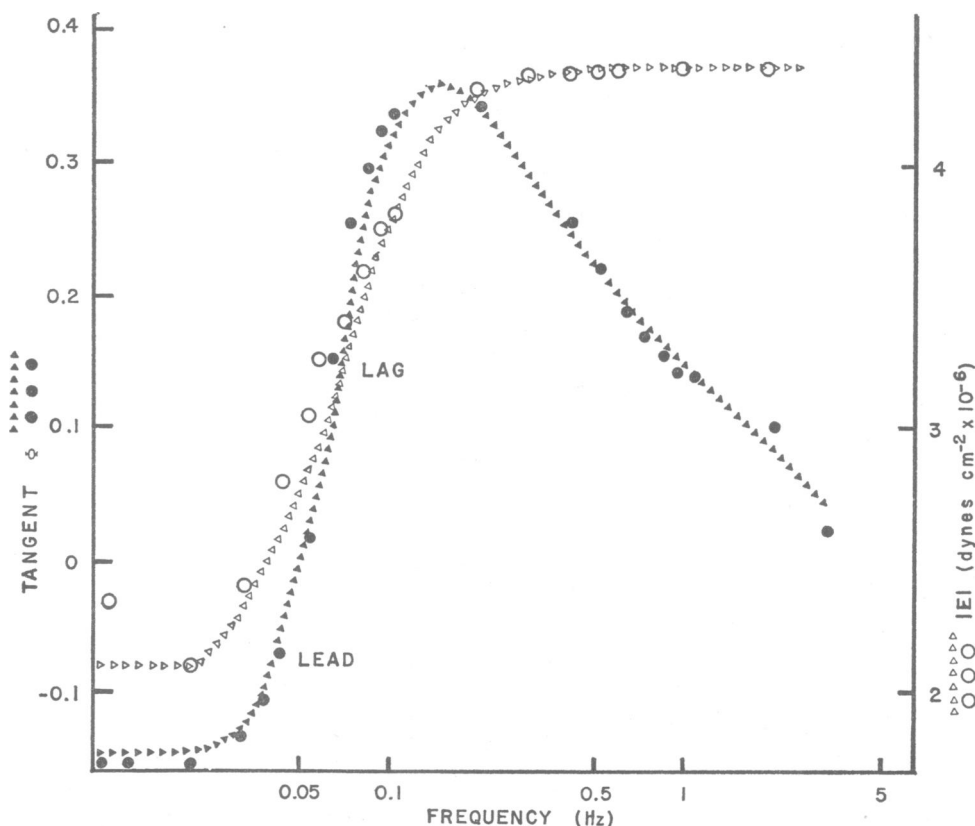


FIGURE 10 Results of experiments on canine urinary bladder with its muscle viable, but relaxed, and on the present model incorporating parameters obtained from stress-relaxation curves of the same arterial specimen. Data depicted as triangles were computed, and circles were experimentally obtained; filled in circles and triangles are phase shift, and open are elastic modulus. The real data differs from the computed primarily in the larger modulus at the lowest frequency of 0.01 Hz. This may reflect elastic modulus enhancement of muscle after one or two oscillations at this low frequency. While the model also showed modulus enhancement after several oscillations, the graph plotted the modulus after one oscillation. The agreement with experimental data is satisfactory since the standard deviation of such measurements can be about 0.53×10^6 dynes cm^{-2} and 0.06 for tangent ϕ (Apter et al., 1966). A similarly good fit was obtained with data from pulmonary artery. However, the fit might be even better if more sophisticated methods (Taylor and Brown, 1965; Wilson, Apter, and Schwartz, 1970) were used to obtain E_1 , E_2 , η and the k_i . See Apter and Marquez (1968 b) for details on use of stress-relaxation curves to obtain model parameters.

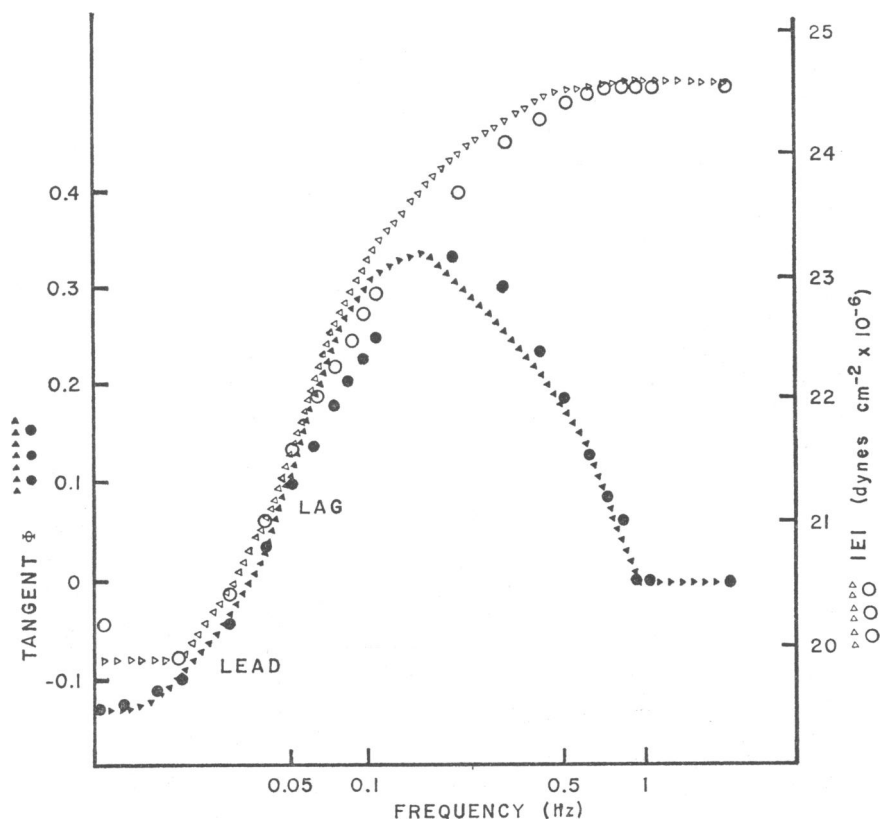


FIGURE 11 The experimental data were obtained from the same specimen as in Figs. 9 and 10 after the addition of sufficient bethanechol hydrochloride to raise the mean tension to a new level about twice as high and reduce the lumen circumference. The strain and stress were computed in accordance with the new dimensions. Analysis of results is as in Fig. 10. The modulus is generally higher and the phase lead angle is larger at low frequencies.

in pulmonary artery specimens. The model also reproduced force-velocity curves and isometric tension development of striated muscle (Fig. 12) although only qualitative comparisons were possible in this case. The time course of the tension response to a step-function change in temperature, the steady-state temperature-tension relationship of smooth muscle (Fig. 13), and the frequency dependence of phase shift and elastic modulus enhancement of smooth (Fig. 5 and 7) and striated (Fig. 12) muscles in general were also computed. The parameter set in each case was chosen solely from the response of that particular kind of muscle to a step-function increase in length.

The model was able to reproduce the thermal response of smooth muscle. A step-function increase in temperature was simulated by imposing a step-function increase in all k_i ($i = 1, \dots, 6$) such that $\Delta k_3 > \Delta k_2 > \Delta k_1 = \Delta k_4 = \Delta k_5 = \Delta k_6$. It would be reasonable for the change in k_2 to be less than the change in k_3 if

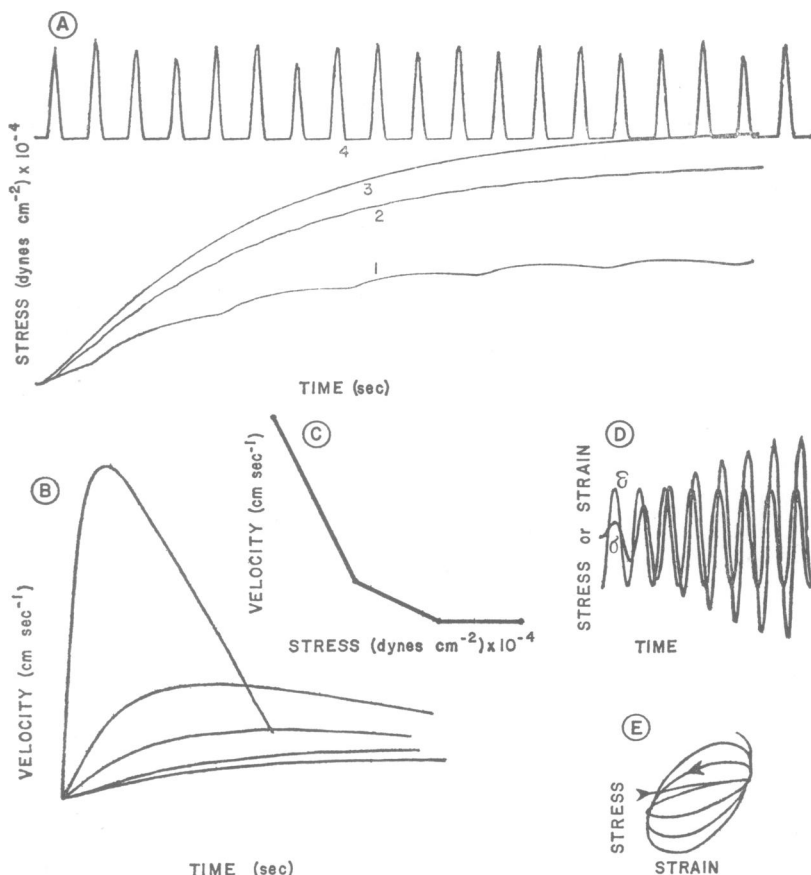


FIGURE 12 Stress response of the model when parameters were chosen to make the model behave like striated muscle (see Table I for parameter values). (A) Response resulting from repetitive stimulation imposed at low (curve 1), intermediate (curve 2), and high (curve 3) frequencies. The N curve (No. 4) is at the frequency used to generate the force-development curve 2. (Compare the results of Buller and Lewis, 1965.) (B) Velocity-time curves obtained by stretching the muscle with a given force, then letting N rise very rapidly ($k_7 = 100$) from t_0 until t_1 . The muscle shortened with the indicated velocities. (Compare the results of Fenn and Marsh, 1935 and Wilkie, 1949.) (C) Force-velocity curves obtained by plotting the maximum velocity in curves (B) versus the force opposing the shortening. (Compare the results of Fenn and Marsh, 1935.) (D), (E) Response of stress to sinusoidal strain resembles "contracted smooth muscle" in Fig. 7.

k_2 reflected diffusion alone while other rate constants reflected enzyme activity. According to the model, a muscle kept under tension at a constant length and exposed to a rise in temperature shows an initial rise in mean stress. However, the steady-state level of N is lower, resulting finally in a net decrease in steady-state tension. A decrease in temperature reverses these events. The calculated results are depicted in Fig. 13, which also shows the results of experiments on the iris sphincter

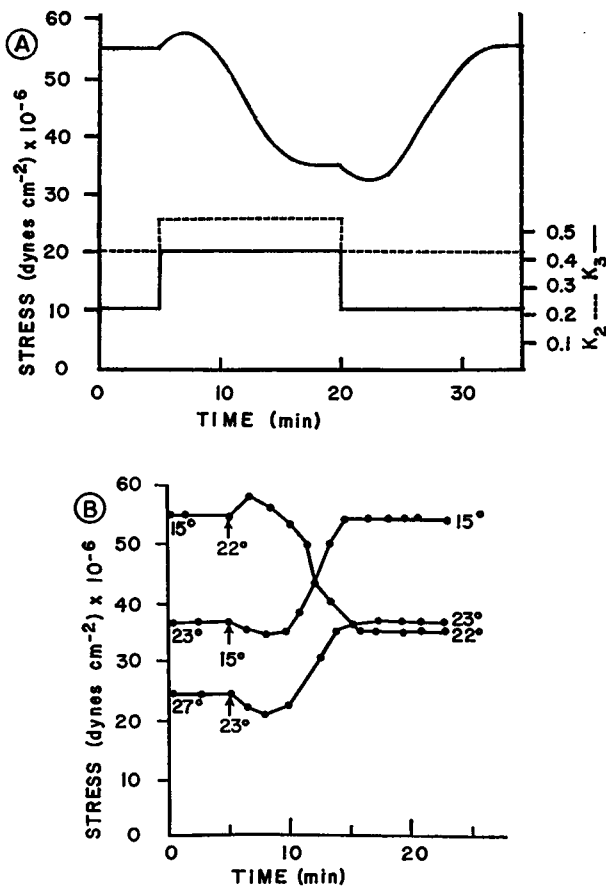


FIGURE 13 (A) Stress response of model to a step-function change in temperature, first an increase, then a decrease. Temperature increase was formalized as an increase in all k_i ($i = 1, \dots, 6$). Parameters were chosen to be consistent with the behavior of smooth muscle in the presence of chemical mediators (see Table I for all parameter values at 0° and 37°C). (B) Response of dog iris sphincter in the presence of acetylcholine to a step-function increase, then decrease, in temperature, showing qualitative similarity to model.

of a dog eye. These resemble data for other smooth muscles which have already been published (Apter, 1961; Apter and Marquez, 1968 *a* and *b*).

DISCUSSION

The model quantitatively reproduced the frequency-dependence of dynamic elastic modulus and phase angle for arterial smooth muscle in the relaxed, contracted, and unviable states, provided model parameters were estimated from experimental stress-relaxation curves of the same specimens. The relationship between stress-relaxation and the frequency analysis is well established in linear viscoelastic sys-

tems, but the nonlinearities of muscle response caused failure in previously available models (Apter and Marquez, 1968 *b*). The ability of a single model to reproduce a wide range of the behavior in a variety of muscles, even qualitatively, is unprecedented. Besides being potentially useful in analyzing other types of experiments, such as force-velocity measurements, the model strongly suggests an underlying similarity in behavior among a wide variety of muscles.

The model has called attention to and clarified the possible reasons for the unique phase lead angle found in muscle and suggests experiments that might establish the factors responsible. For example, how do temperature or ionic environments influence model parameters measured from phase angles? The model also establishes the reasonable coexistence of a phase lead angle with elastic modulus enhancement and of phase lag with stress-relaxation during an oscillation. The phase lead implies energy production and a higher elastic modulus; phase lag implies dissipation and a consequent lower modulus.

The model failed in some instances to match real behavior. Like all other models, it did not follow the detailed time course of the velocity of shortening. In particular, there was none of the delay that precedes shortening of a stimulated muscle. This discrepancy probably results from a failure of the model to include a finite time interval before the presence of N can induce reorientation of macromolecules. The model does not attempt to represent the behavior of muscle in a very highly stretched state, and thus, for example, could not reproduce the entire length-active tension relationship (Huxley, 1963). This would restrict the utility of the model if it were presented as a theory of muscular contraction, but does not limit its utility for the present purposes. The ability of the model to reproduce spontaneous "muscular" activity has not been tested. However, since stress-amplification occurs only at particular frequencies of forced oscillation, and in real muscle particularly at the frequency of spontaneous oscillations (Ruegg, 1968; Apter and Graessley, 1969), this point deserves further study with this model. Future work will include a search for other types of muscular behavior amenable to quantitative analysis and a careful examination of the ranges and limits on the values of the model parameters (Taylor and Brown, 1965; Wilson, Apter and Schwartz, 1970).

GLOSSARY OF UNITS

k_i	($i = 1, 4, 5, 6$) ($\text{cm}^3 \text{g}^{-1}$)
k_2, k_7	($\text{g cm}^{-3} \text{sec}^{-1}$)
k_3	(sec^{-1})
E_1, E_2	elastic moduli (dynes cm^{-2})
η	viscosity coefficient (poise cm^{-2})
l_0, l	length (cm)
σ	stress (dynes cm^{-2})
ϵ	strain dimensionless
t	time (sec)
v	velocity (cm sec^{-1})

F	force (dynes)
$\dot{\epsilon}$	strain rate (sec^{-1})
$\dot{\sigma}$	stress rate ($\text{dynes cm}^{-2} \text{ sec}^{-1}$)
n	concentration (g cm^{-3})
\dot{n}	rate of change of concentration ($\text{g cm}^{-3} \text{ sec}^{-1}$)

This work was supported in part by USPHS grants GM-14659, HE-05808, and CA-06475.

Received for publication 26 September 1969 and in revised form 8 January 1970.

REFERENCES

- APTER, J. T. 1961. *Amer. J. Ophthalmol.* **51** (2):1141/269.
- APTER, J. T., and W. W. GRAESSLEY. 1969. *Experientia (Basel)*. **25**:145.
- APTER, J. T., and E. MARQUEZ. 1968 *a*. *Circ. Res.* **22**:393.
- APTER, J. T., and E. MARQUEZ. 1968 *b*. *Biorheology*. **5**:285.
- APTER, J. T., and H. NAJAFI. 1968. *J. Amer. Med. Ass.* **206**:2881.
- APTER, J. T., M. RABINOWITZ, and D. H. CUMMINGS. 1966. *Circ. Res.* **19**:104.
- BAHLER, A. S. 1968. *I.E.E.E. (Inst. Elec. Electron Eng.) Trans. Bio-Med. Eng.* **15**:249.
- BULLER, A. J., and D. M. LEWIS. 1965. *J. Physiol. (London)*. **176**:337.
- FENN, W. O., and B. S. MARSH. 1935. *J. Physiol. (London)*. **85**:277.
- HILL, A. V. 1938. *Proc. Roy. Soc. Ser. B. Biol. Sci.* **126**:136.
- HUXLEY, H. E. 1957. *Progr. Biophys. Mol. Biol.* **7**:255.
- HUXLEY, H. E. 1963. *J. Mol. Biol.* **7**:281.
- KOLSKY, H. 1960. In International Symposium on Stress Wave Propagation in Material. N. Davies, editor. Interscience Publishers, Inc., New York. 59-89.
- RAMSEY, R. W., and S. F. STREET. 1940. *J. Cell. Comp. Physiol.* **15**:11.
- RUEGG, J. C. 1968. *Experientia (Basel)*. **24**:529.
- SANDOW, A. 1965. *Pharmacol. Rev.* **17**:265.
- STAVERMAN, A. J., and F. R. SCHWARZL. 1956. Linear Deformation Behavior of High Polymers in Die Physik der Hochpolymeren. H. A. Stuart, editor. Springer-Verlag OHG, Berlin. **4**:1.
- TAYLOR, R. I., and T. H. BROWN. 1965. *J. Phys. Chem.* **69**:2316.
- TOBOLSKY, A. V. 1960. Properties and Structure of Polymers. John Wiley and Sons, Inc., New York. 65.
- VICKERS, W. H., and T. B. SHERIDAN. 1968. *I.E.E.E. (Inst. Elec. Electron Eng.) Trans. Man-Mach. Syst.* **9**:21.
- WILSON, D., J. T. APTER, and F. D. SCHWARTZ. 1970. *J. Appl. Physiol.* **28**:79-88.
- WILKIE, D. R. 1949. *J. Physiol. (London)*. **110**:249.